

Electronic supplementary information

SUPRAMOLECULAR NANOCONTAINER WITH THE MITOCHONDRIA-TARGETING FUNCTION BASED ON A CALIXRESORCINE CAVITAND

Y. E. Morozova,^{*a} A. M. Shumatbaeva,^b Z. R. Gilmullina,^a A. P. Lyubina,^a
S. K. Amerhanova,^a A. D. Voloshina,^a V. V. Syakaev,^a and I. S. Antipin^b

^a *Arbuzov Institute of Organic and Physical Chemistry, FRC Kazan Scientific Center
of the Russian Academy of Sciences, ul. Arbuzova 8, Kazan, 420088 Russia*

^b *Kazan Federal University, ul. Kremlevskaya 18, Kazan, 420008 Russia*

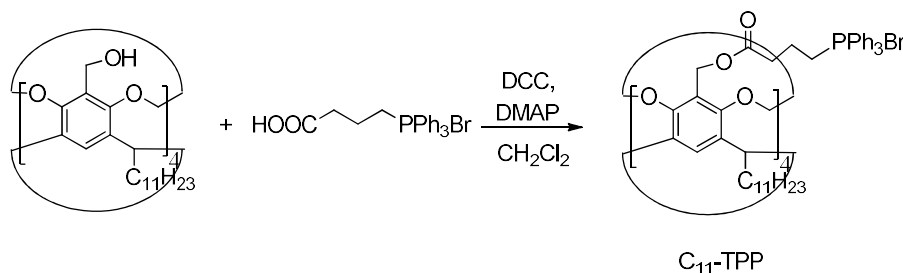
Table of contents

1. Materials and methods	S2
1.1. Synthesis of C ₁₁ -TPP	S2
Figure S1. ¹ H NMR spectrum of C ₁₁ -TPP in DMSO- <i>d</i> ₆	S3
Figure S2. ¹³ C NMR spectrum of C ₁₁ -TPP in DMSO- <i>d</i> ₆	S3
Figure S3. IR spectra of C ₁₁ -TPP (KBr), C ₁₁ -TPP+PAA (KBr) and 25 % aq. PAA (CaF ₂).	S4
1.2. Methods.....	S4
1.2.1. Preparation of the polymer complex solutions by Job's method	S5
Table S1. Concentrations of components in C ₁₁ -TPP–PAA solutions	S5
Figure S4. Intensity particle size distribution curves in PAA and C ₁₁ -TPP+PAA solutions in DMSO–H ₂ O (5/95 v/v).	S6
Figure S5. Zeta potential distribution curves for PAA and C ₁₁ -TPP+PAA solutions in DMSO–H ₂ O (5/95 v/v).	S7
Figure S6. Average values of hydrodynamic diameter (<i>a</i>) and electrokinetic potential (<i>b</i>) of the particles of the polymer complex solutions at different concentrations of C ₁₁ -TPP.....	S8
1.2.2. Preparation of the samples for IR spectroscopic studies.....	S8
Figure S7. Pyrene (0.001 mM) fluorescence spectra in the presence of C ₁₁ -TPP in DMSO/H ₂ O (5/95 v/v) solutions in the absence (<i>a</i>) and presence (<i>b</i>) of PAA (0.5 mM).	S8
Figure S8. Dependence of I/III of pyrene on log <i>C</i> of C ₁₁ -TPP in the individual solution and in the presence of PAA in DMSO–H ₂ O (5/95 v/v).	S9
Figure S9. Dependence of the electrical conductivity on C ₁₁ -TPP concentration in the individual solution (<i>a</i>) and in the presence of 0.5 mM PAA (<i>b</i>) in DMSO–H ₂ O (5/95 v/v).	S9
1.2.3. Preparation of C ₁₁ -TPP+PAA+FI complex and investigation of the FI release	S9
Figure S10. Percentage of the FI release from C ₁₁ -TPP+PAA complex (the dialysis method, dialysate: 0.1 % Tween-20 in DMSO–PB (5/95 v/v), pH 7.4).	S10
1.2.4. Hemolytic activity assay and cytotoxicity studies of C ₁₁ -TPP, PAA, and the resulting complex..	S10
1.2.5. Mitochondrial membrane potential investigation.....	S11
Figure S11. Data of flow cytometry analysis of <i>M-HeLa</i> cells, treated with the studied samples.....	S11
2. Literature data on the mitochondria-targeted systems based on cucurbiturils and cyclodextrins	S11
References.....	S12

1. Materials and methods

PAA with M_w of 240.0 kDa was obtained from Aesar (25% aq.). *N,N'*-Dicyclohexylcarbodiimide (DCC) and 3-(carboxypropyl)triphenylphosphonium bromide were obtained from Aldrich, and 4-dimethylaminopyridine (DMAP) was obtained from Acros. Tetraundecyl-hydroxycavitand was synthesized according to the published procedure [1]. The molar concentrations of PAA in the solutions were calculated from the monomer mass and corresponded to the number of moles of monomer units per 1000 mL of the solution.

1.1. Synthesis of C₁₁-TPP



Tetraundecyl-hydroxycavitand (1.004 g, 0.79 mmol) was dissolved in 50 mL of dry dichloromethane. Then a solution of DCC (0.846 g, 2.5 mmol) in 25 mL of dry CH₂Cl₂ and the catalytic amount of DMAP (0.005 g) were added. The reaction mixture was cooled to 9 °C, and 3-(carboxypropyl)triphenylphosphonium bromide (1.76 g, 0.41 mmol) was added. The reaction mixture was stirred at room temperature under an inert atmosphere for 48 h. The resulting precipitate was filtered off, and filtrate was evaporated. The residue was dissolved in 100 mL of CH₂Cl₂, and the newly formed precipitate was filtered off. The solution was sequentially washed with 0.5 M HCl and saturated aq. NaHCO₃ (×3). The organic phase was separated and dried over MgSO₄. The solvent was evaporated, and the residue obtained was dried under reduced pressure to give C₁₁-TPP as a white solid. Yield: 1.885 g (80%). $T_{dec} = 233.4$ °C.

¹H NMR (DMSO-*d*₆, 500 MHz): δ 0.84 (t, 12H, $J = 8$ Hz), 1.36–1.22 (m, 64H), 1.71–1.70 (m, 8H), 2.36–2.31 (m, 8H), 2.59 (m, 8H), 3.72–3.43 (m, 8H), 3.94–3.73 (m, 8H), 4.39–4.21 (m, 4H), 4.57 (q, 4H, $J = 8$ Hz), 4.83 (s, 8H), 5.83–5.66 (m, 4H), 7.86–7.60 (m, 64H). ¹³C NMR (DMSO-*d*₆, 126 MHz): δ 171.8 (s, C12), 153.4 (s, C2), 137.8 (s, C3), 134.7 (s, C19), 133.6 (s, C17), 130.1 (s, C18), 122.1 (s, C4), 118.4 (s, C1 and C16), 99.4 (s, C10), 56.2 (s, C11), 36.8 (s, C5), 32.9 (s, C13), 31.3 (s, C8), 29.2 (s, C6 and C15), 28.7 (s, C7), 22.0 (s, C8), 19.4 (s, C14), 13.8 (s, C9). IR (KBr): 2925, 2854 s (ν_{CH}); 1728 s ($\nu_{C=O}$), 1665, 1638 s ($\nu_{C=Ar}$). Anal. Calcd for C₁₆₈H₂₀₀Br₄N₄O₁₆P₄: C, 69.13; H, 6.91; Br, 10.95; P, 4.24. Found: C 69.23; H 7.04; Br 10.73; P 4.28 %.

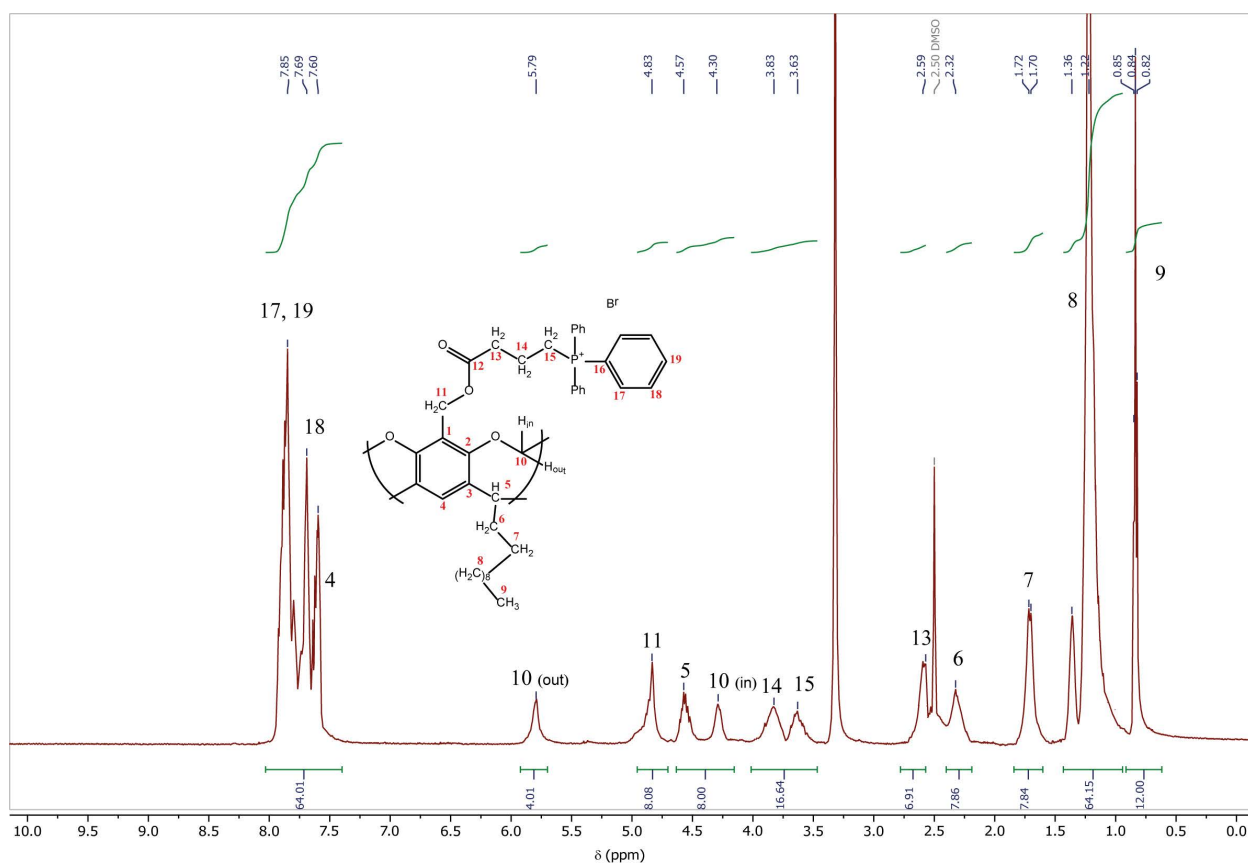


Figure S1. ¹H NMR spectrum of C₁₁-TPP in DMSO-*d*₆.

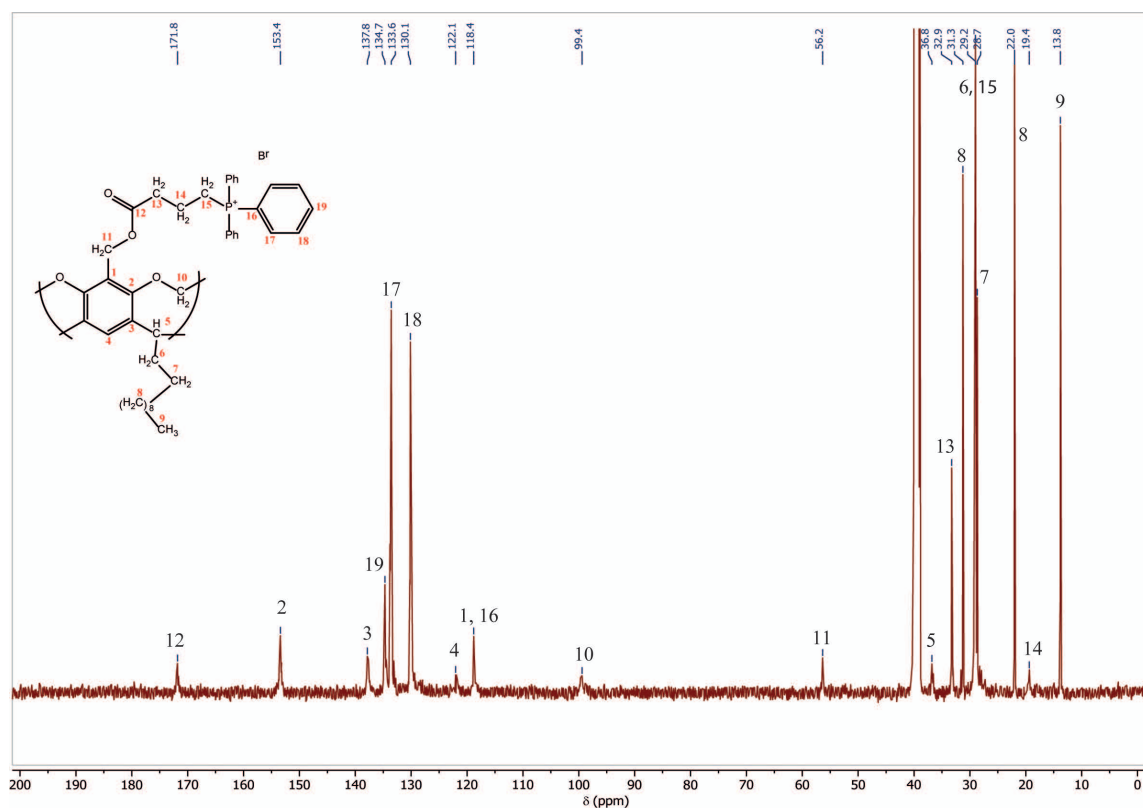


Figure S2. ¹³C NMR spectrum of C₁₁-TPP in DMSO-*d*₆.

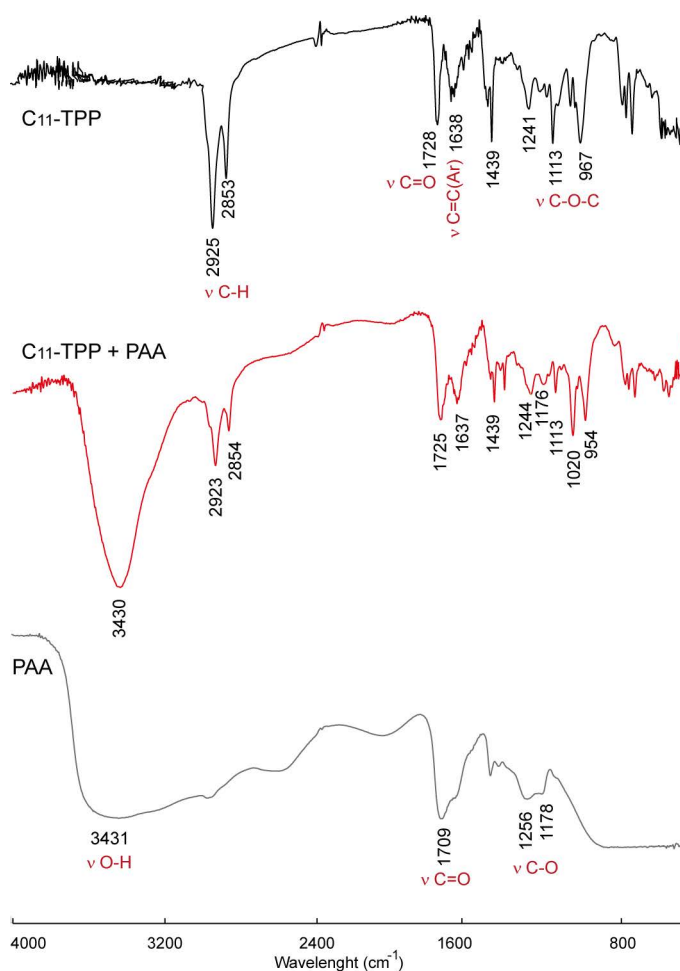


Figure S3. IR spectra of C₁₁-TPP (KBr), C₁₁-TPP+PAA (KBr) and 25 % aq. PAA (CaF₂).

1.2. Methods

All NMR experiments were performed on a Bruker AVANCE(III)-500 spectrometer. The spectrometer was equipped with a Bruker multinuclear z-gradient inverse probe head capable of producing gradients with a strength of 50 G cm⁻¹. All experiments were carried out at 303 ± 0.1 K. The ¹H NMR data were recorded in DMSO-*d*₆ using residual CD₃S(O)CD₂H (δ = 2.5) as an internal standard.

The IR spectra were recorded using a Vector-27 IR spectrometer (Bruker, Germany) in KBr or CaF₂ pellets. The elemental analysis was carried out on a Vario Macro cube CHNS analyzer (Elementar Analysensysteme GmbH, Germany). The UV-Vis spectra were registered on a Lambda 35 UV/VIS Spectrometer (Perkin Elmer Instruments).

The TGA/DSC measurements were carried out with a Netzsch STA 449C Jupiter instrument in argon in the temperature range from 30 to 550 °C. The heating rate was 10 deg/min. The sample was placed in aluminum crucibles (non-sealed for the free removal of evolved products and a decrease of the influence of an excessive pressure).

The DLS measurements were carried out on a Zetasizer Nano-ZS (MALVERN) instrument using Dispersion Technology Software 5.00. Each solution was tested at least three times. The error of hydrodynamic particle size determination was 2%. A Zeta potential Nano-ZS (MALVERN) with laser Doppler velocimetry and phase analysis of light scattering was used for zeta potential measurements by the electrophoretic light scattering method. The measurements were carried out in folded capillary cells (DTS1061, Malvern). The temperature of the scattering cell was controlled at 25 °C. The data were analyzed using the software supplied for the instrument.

The electrical conductivities were measured using a Toledo FE-30 precision conductivity meter at 25 °C. The solutions of C₁₁-TPP in DMSO/H₂O (5/95 v/v) in the absence and in the presence of 0.5 M solution of PAA in DMSO/H₂O (5/95 v/v) were prepared by the dilution method; the dilution was made using DMSO/H₂O (5/95 v/v) or 0.5 M PAA solution in DMSO/H₂O (5/95 v/v), respectively. The conductivity of each solution was measured three times to obtain an average value; the concentration range was 0.045–0.25 mM.

The fluorescence spectra were recorded on a Hitachi F-7100 fluorescence spectrophotometer in a 1 cm quartz cells at 25 °C. The excitation wavelength of pyrene (0.001 mM) was set at 333 nm, and the emission range was from 345 to 500 nm; the ratio of the first (372 nm) and third (381 nm) emission bands I/III for every spectrum was estimated, and the CAC values were graphically determined from the sigmoidal plots of the I/III ratio vs. the logarithm of macrocycles concentration according to Ref. [2]. The solutions of C₁₁-TPP in DMSO/H₂O (5/95 v/v) in the absence and in the presence of 0.5 M solution of PAA in DMSO/H₂O (5/95 v/v) were prepared by the dilution method, the dilution was made using DMSO/H₂O (5/95 v/v) or 0.5 M PAA solution in DMSO/H₂O (5/95 v/v), respectively. The excitation wavelength of fluorescein was 491 nm.

1.2.1. Preparation of the polymer complex solutions by Job's method

The initial solutions of PAA and C₁₁-TPP were prepared in DMSO/H₂O (5/95 v/v) with the concentrations of 0.005 M and 0.5 M, respectively. Using the data from Table S1, the solutions were prepared by adding aliquots of PAA solution to the corresponding volumes of DMSO and H₂O upon stirring at 360 rpm. Then the corresponding aliquot of C₁₁-TPP solution was added upon stirring, and the solutions were stirred for 1 h. The resulting solutions were used for the DLS measurements.

Table S1. Concentrations of components in C₁₁-TPP–PAA solutions

NN	V_{common} , mL	Fraction of C ₁₁ -TPP	Fraction of PAA	$C_{\text{C11-TPP}}$, M	C_{PAA} , M	$V_{\text{aliquot of C11-TPP solution}}$, mL	$V_{\text{aliquot of PAA solution}}$, mL	V_{DMSO} , mL	V_{H2O} , mL
1	2	0.1	0.9	1.0E-04	9.0E-04	0.004	0.360	0.1	1.536
2	2	0.2	0.8	2.0E-04	8.0E-04	0.008	0.320	0.1	1.572
3	2	0.3	0.7	3.0E-04	7.0E-04	0.012	0.280	0.1	1.608
4	2	0.4	0.6	4.0E-04	6.0E-04	0.016	0.240	0.1	1.644
5	2	0.5	0.5	5.0E-04	5.0E-04	0.020	0.200	0.1	1.680
6	2	0.6	0.4	6.0E-04	4.0E-04	0.024	0.160	0.1	1.716
7	2	0.7	0.3	7.0E-04	3.0E-04	0.028	0.120	0.1	1.752
8	2	0.8	0.2	8.0E-04	2.0E-04	0.032	0.080	0.1	1.788
9	2	0.9	0.1	9.0E-04	1.0E-04	0.036	0.040	0.1	1.824
PAA	2	0	1	0	1.0E-03	0	0.400	0.1	1.500
C ₁₁ -TPP	2	1	0	1.0E-03	0	0.040	0	0.1	1.860

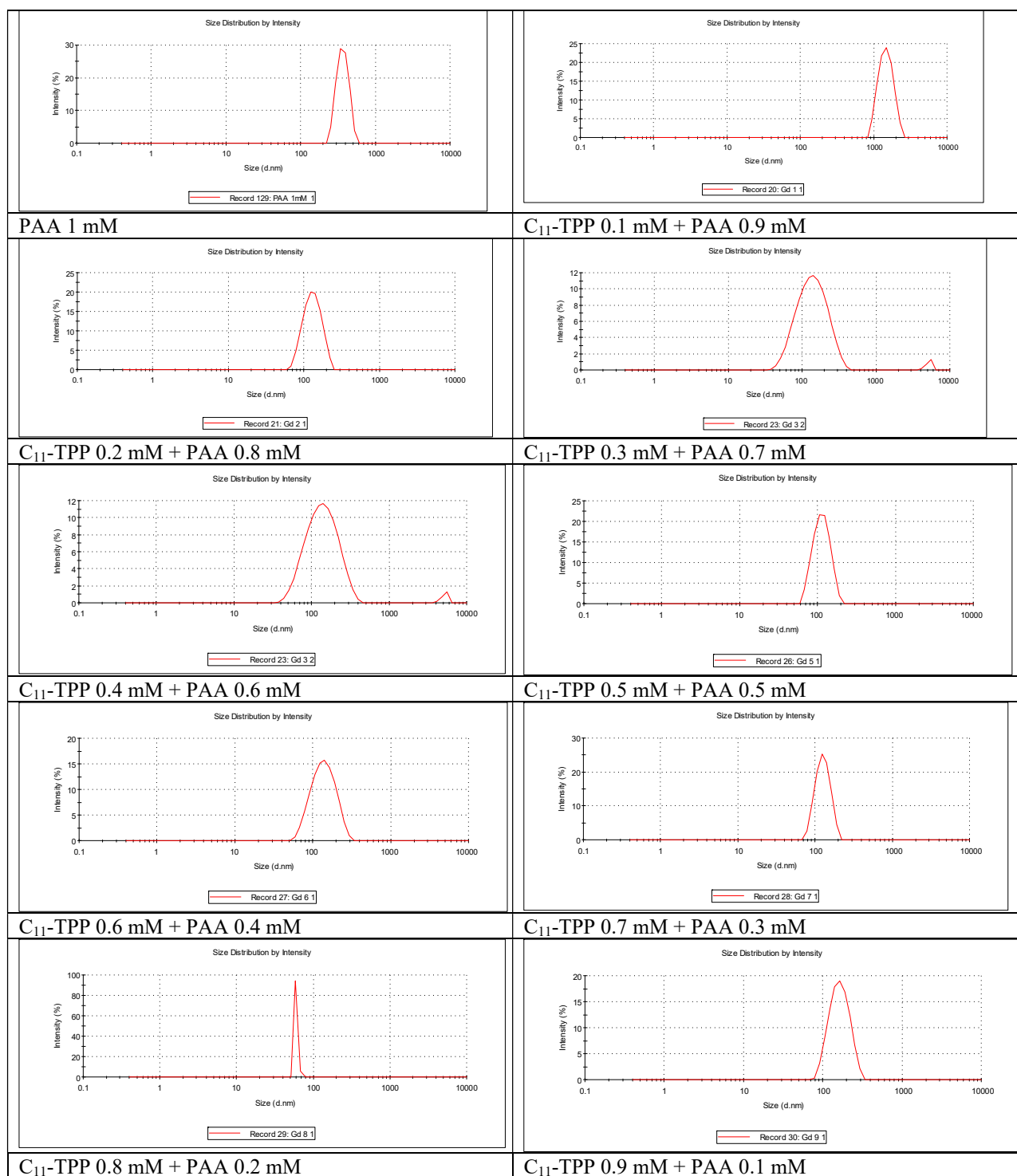


Figure S4. Intensity particle size distribution curves in PAA and C₁₁-TPP+PAA solutions in DMSO–H₂O (5/95 v/v).

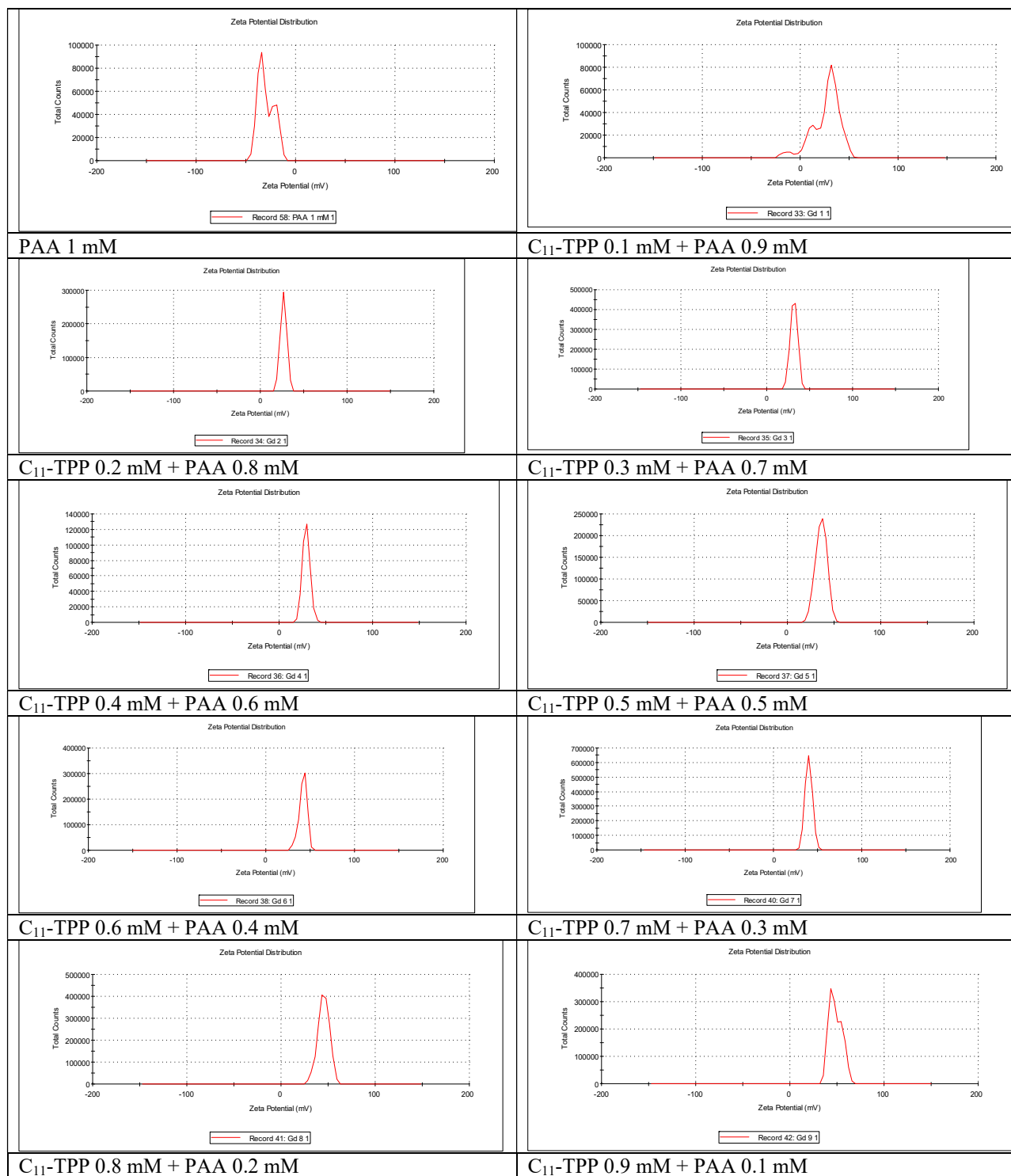


Figure S5. Zeta potential distribution curves for PAA and C₁₁-TPP+PAA solutions in DMSO–H₂O (5/95 v/v).

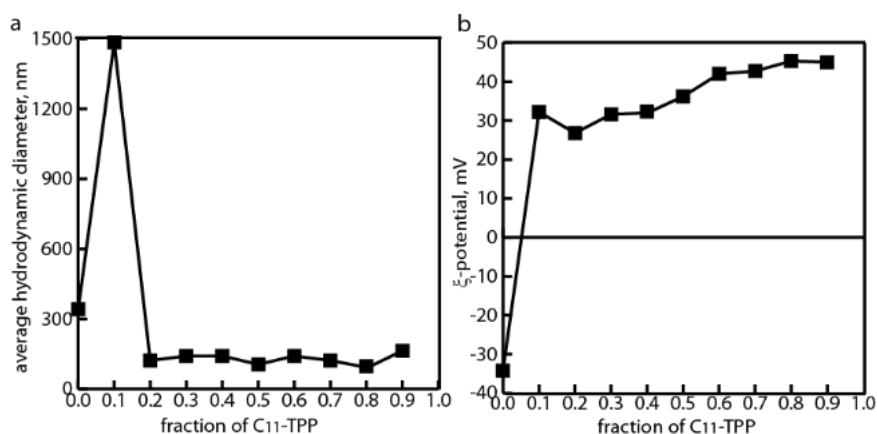


Figure S6. Average values of hydrodynamic diameter (*a*) and electrokinetic potential (*b*) of the particles of the polymer complex solutions at different concentrations of C₁₁-TPP.

1.2.2. Preparation of the samples for IR spectroscopic studies

The IR spectrum of PAA was recorded using 25 % aq. PAA in a CaF₂ pellet. A sample of C₁₁-TPP–PAA complex was prepared by addition of 0.13 mL of 0.05 M aq. solution of PAA to 12.74 mL of bidistilled H₂O. Then 0.13 mL of 0.05 M solution of C₁₁-TPP in DMSO was added upon stirring, and the resulting mixture was stirred at 360 rpm for 30 min. After that, the solution was centrifuged at 6000 rpm for 10 min, and the resulting precipitate was dried using molecular sieves A4 for 72 h. The IR spectrum of the sample was recorded in a KBr pellet.

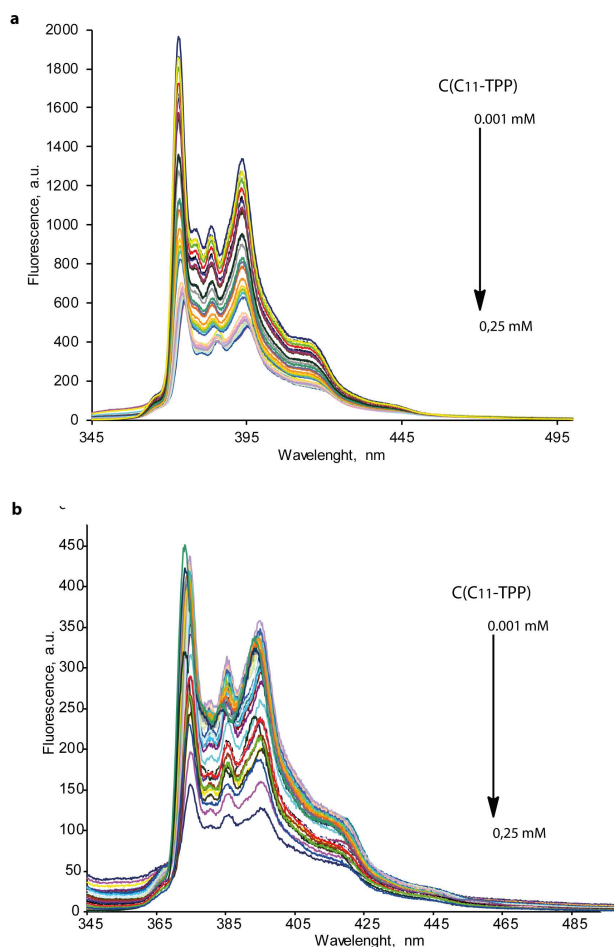


Figure S7. Pyrene (0.001 mM) fluorescence spectra in the presence of C₁₁-TPP in DMSO/H₂O (5/95 v/v) solutions in the absence (*a*) and presence (*b*) of PAA (0.5 mM).

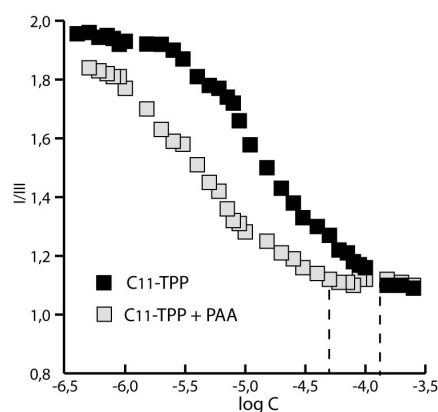


Figure S8. Dependence of I/III of pyrene on $\log C$ of C_{11} -TPP in the individual solution and in the presence of PAA in DMSO–H₂O (5/95 v/v).

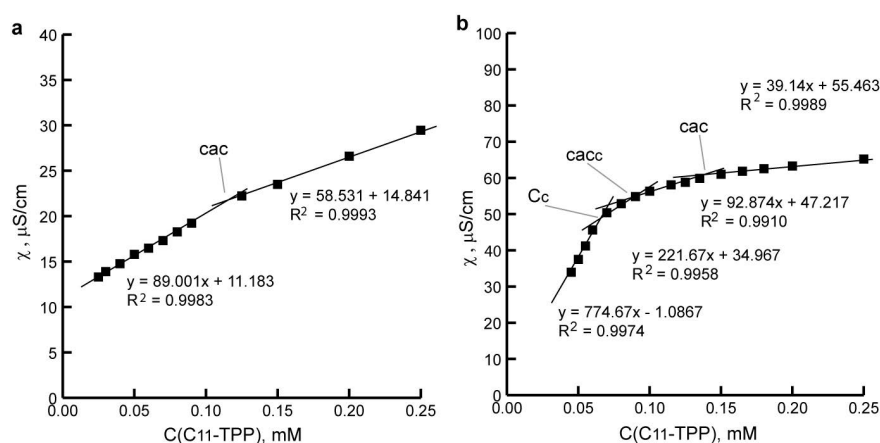


Figure S9. Dependence of the electrical conductivity on C_{11} -TPP concentration in the individual solution (**a**) and in the presence of 0.5 mM PAA (**b**) in DMSO–H₂O (5/95 v/v).

The critical association concentration (cac) of C_{11} -TPP in the individual solution was found to be 0.095 mM (fluorimetry method with pyrene) and 0.12 mM (conductometry) (Figs. S8, S9a). The lower cac value obtained by the pyrene method can be explained by an increase in the self-association of the cavitand in the presence of the solubilized dye.

On the conductivity isotherm of C_{11} -TPP in PAA solution, three critical points can be observed (C_c , cac_c , and cac) (Fig. S9). According to Ref. [3], C_c represents the point at which the surfactant monomers adsorbed onto the polymer chains, cac_c is the point where surfactant self-associates begin to form on the polymer chain, while cac is reached when self-associates of the surfactant start to form in the solution. The estimated values for C_c , cac_c , and cac are 0.065, 0.095, and 0.153 mM, respectively. It can be seen that the value of C_c is close to the cac value obtained by the fluorimetry method. This suggests that the adsorption on the polymer chain is accompanied by the dimerization of the cavitand molecules, while at the cac_c point further association may occur. Moreover, the presence of PAA leads to an increase in C_{11} -TPP cac value (from 0.120 to 0.153 mM), indicating a strong affinity of the cavitand molecules to the PAA surface. Based on these data, it can be proposed that at 0.5/0.5 C_{11} -TPP/PAA molar ratio, the cavitand self-associates adsorb on PAA molecules due to electrostatic interactions (Fig. 2b).

1.2.3. Preparation of C_{11} -TPP+PAA+Fl complex and investigation of the Fl release

The solution of C_{11} -TPP+Fl in DMSO was prepared with $C(C_{11}\text{-TPP}) = C(\text{Fl}) = 0.05$ M. Then the solution of C_{11} -TPP+PAA+Fl (5 mL) was obtained with an aliquot of C_{11} -TPP+Fl solution and an aliquot of 5 mM PAA solution in H₂O/DMSO 95/5 v/v; $C(C_{11}\text{-TPP}) = C(\text{Fl}) = C(\text{PAA}) = 0.5$ mM. The solution was dialyzed against H₂O/DMSO 95/5 v/v for 3 h (3.5 kDa, 25° C). The concentration of Fl was

estimated by spectrophotometry method at λ_{\max} 482 nm ($\varepsilon = 92300 \text{ cm}^{-1}$). The encapsulation effectiveness (EE) and drug loading (DL) values were obtained using the following equations

$$EE = 100\% \cdot C_c/C_0,$$

$$DL = 100\% \cdot m(FI)/m_c,$$

where C_0 and C_c are the initial concentration of FI and the concentration in the complex, respectively; $m(FI)$ и m_c are the mass of FI and the mass of the complex (g), respectively. The values were found to be 98 and 0.61 %, respectively.

Then, for release profile study, 2 mL of the C_{11} -TPP+PAA+FI solution was diluted to 5 mL with H_2O /DMSO 95/5 v/v solution and it was dialyzed against 500 mL of 0.1% Tween solution in PB(pH 7.4)/DMSO 95/5 v/v mixture (3.5 kDa, 25° C). 3 mL of phase was replaced each 15–20 min with fresh solution and was analyzed by fluorimetry.

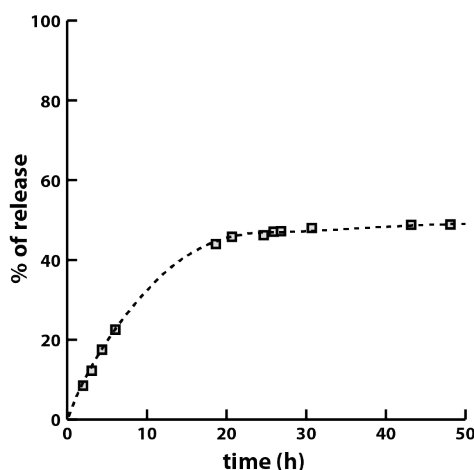


Figure S10. Percentage of the FI release from C_{11} -TPP+PAA complex (the dialysis method, dialysate: 0.1 % Tween-20 in DMSO–PB (5/95 v/v), pH 7.4).

1.2.4. Hemolytic activity assay and cytotoxicity studies of C_{11} -TPP, PAA, and the resulting complex

Hemolytic activity assay. Fresh hRBC with heparin were rinsed 3 times with 0.15 M NaCl by centrifugation at 800 rpm for 10 min and re-suspended in 0.15 M NaCl. Each of the investigated solutions in 0.15 M NaCl was then added to 0.5 mL of a solution of the stock hRBC in 0.15 M NaCl to reach a final volume of 5 mL (final erythrocyte concentration 10% v/v). The resulting suspension was incubated under agitation for 1 h at 37 °C. The samples were then centrifuged at 2000 rpm for 10 min. The release of hemoglobin was monitored by measuring the absorbance of the supernatant at 540 nm by means of an AP-101 digital photoelectric colorimeter (Apel, Japan). Controls for zero hemolysis (blank) and 100% hemolysis consisted of hRBC which was suspended in 0.15 M NaCl and bidistilled water, respectively.

Cytotoxicity studies. The cytotoxic effects on cells were determined using the MTT colorimetric method. Chang liver and M-HeLa clone 11 cells were seeded on a 96-well Nunc plate at a concentration of 5×10^3 cells per well in a volume of 100 μ L of medium and cultured in a CO_2 incubator at 37 °C until a monolayer was formed. Then the nutrient medium was removed and 100 μ L of solutions of the test compound at specified dilutions were added to the wells prepared directly in the nutrient medium with the addition of DMSO (5% by volume) to improve the solubility of the compounds in the stock solution. The concentration of DMSO in the experimental wells did not exceed 1%. After 48 h incubation of cells with the tested compounds, the nutrient medium was removed from the plates, and 100 μ L of the nutrient medium without serum containing MTT at a concentration of 0.5 mg/mL was added and incubated for 4 h at 37 °C. Formazan crystals were added 100 μ L of DMSO to each well. Absorbance was recorded at 540 nm on an Invitrogen microplate reader (Russia). Experiments for all compounds were repeated three times.

Statistical analysis. The values of IC_{50} were calculated using an online tool: MLA-Quest Graph™ IC_{50} Calculator (AAT Bioquest, Inc., <https://www.aatbio.com/tools/ic50-calculator> (accessed on 5 July 2021)).

1.2.5. Mitochondrial membrane potential investigation

M-HeLa cells at 1×10^6 cells/well in a final volume of 2 mL were seeded into six-well plates. After 24 h of incubation, the compounds in concentrations corresponding to IC_{50} and half of IC_{50} were added to the wells. The resulting suspensions as well as the sample without any additional components (control) were incubated for 24 h at 37 °C. The cells were harvested at 2000 rpm for 5 min and then washed twice with ice-cold PBS, followed by resuspension in JC-10 (10 μ g/mL) and incubation at 37 °C for 10 min. After the cells were rinsed three times and suspended in PBS, the JC-10 fluorescence was observed by flow cytometry (Guava easy Cyte, MERCK, USA). The experiments were repeated three times. The results were evaluated by means of multifunctional system Cytell Cell Imaging (GE Healthcare Life Sciences, Sweden) using Cell Viability BioApp application.

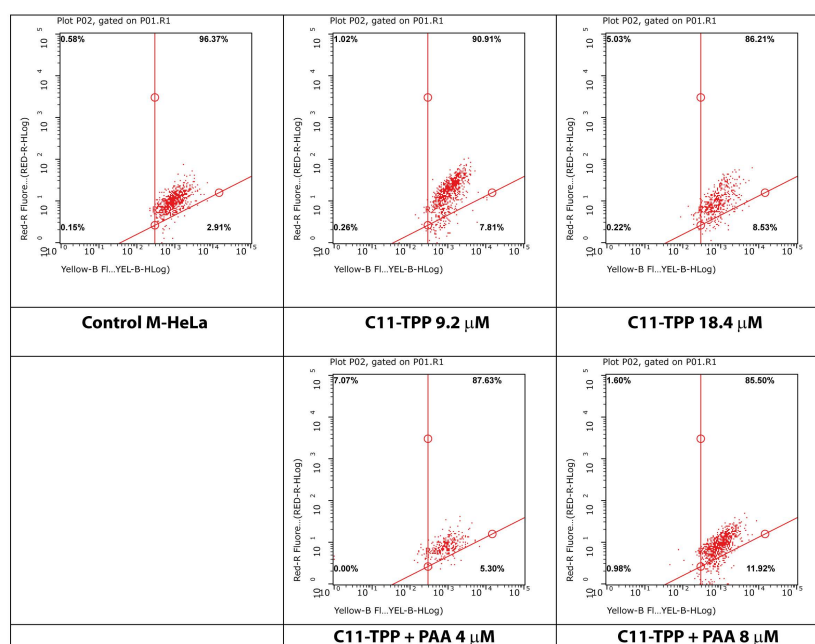


Figure S11. Data of flow cytometry analysis of *M-HeLa* cells, treated with the studied samples.

2. Literature data on the mitochondria-targeted systems based on cucurbiturils and cyclodextrins

Recently, several interesting studies have been published on the design of mitochondria-targeted systems based on supramolecular macrocycles such as cyclodextrins (CDs) and cucurbiturils (CBs). Yamada *et al.* presented polyrotaxanes, created from the inclusion complexes of β -CD with Pluronic P103 molecule, which were functionalized with TPP units [4]. After modification of the complexes with octaarginine and S2 peptide, which have cell uptake and mitochondrial targeting activity, the nanoparticles with a diameter of 100–200 nm were obtained. It was shown that these nanoparticles are able to artificially induce autophagy in cells and organelles [4].

Sun *et al.* reported a supramolecular system that can induce mitochondrial aggregation and fusion. They modified polyethylene glycol with TPP and adamantine moieties and hyaluronic acid with CB. On

the mitochondria surfaces, both compounds exhibited strong host–guest interactions between the CB moiety and adamantine unit, which led to the mitochondrial aggregation [5].

Shen *et al.* developed a supramolecular system for mitochondrial imaging based on β -cyclodextrin-modified hyaluronic acid (CD-HA), CB8 and a tetraphenylethene derivative (TPE) [6]. In the solution, CB8 and TPE form pseudorotaxanes, which aggregates into nanoparticles with the diameter ranging from 200 to 1000 nm. In these pseudorotaxanes, the emission of TPE is enhanced and red-shifted to 680 nm. Further aggregation of CB8–TPE complex with CD-HA leads to the nanoparticles with the diameters of 50 to 300 nm and a stronger dye emission [6].

Zhou *et al.* reported a supramolecular system obtained from CBs and hyaluronic acid, which was modified with 4-(4-bromophenyl)pyridin-1-ium bromide (BrBP) [7]. CB forms a complex with the BrBP moiety that leads to an enhancement in the dye emission. Due to the mitochondrial targeting properties of this supramolecular system, phosphorescence imaging of Hela cells was achieved using a visible light source (488 nm) [7].

References

1. S. Pellet-Rostaing, L. Nicod, F. Chitry, M. Lemaire, *Tetrahedron Lett.*, **1999**, *40*, 8793–8796. DOI: 10.1016/S0040-4039(99)01870-5
2. J. Aguiar, P. Carpena, J. A. Molina-Bolívar, C. C. Ruiz, *J. Colloid Interface Sci.*, **2003**, *258*, 116–122. DOI: 10.1016/S0021-9797(02)00082-6
3. A. Pal, R. Maan, *Colloid Polym. Sci.*, **2018**, *296*, 483–494. DOI: 10.1007/s00396-018-4263-5
4. Y. Yamada, S. Daikuhara, A. Tamura, K. Nishida, N. Yui, H. Harashima, *Chem. Commun.*, **2019**, *55*, 7203–7206. DOI: 10.1039/c9cc03272j
5. C. Sun, Z. Wang, L. Yue, Q. Huang, Q. Cheng, R. Wang, *J. Am. Chem. Soc.*, **2020**, *142*, 16523–16527. DOI: 10.1021/jacs.0c06783
6. F.-F. Shen, Y. Chen, X. Xu, H.-J. Yu, H. Wang, Y. Liu, *Small*, **2021**, *17*, 2101185. DOI: 10.1002/sml.202101185
7. W.-L. Zhou, Y. Chen, Q. Yu, H. Zhang, Z.-X. Liu, X.-Y. Dai, J.-J. Li, Y. Liu, *Nat. Commun.*, **2020**, *11*, 4655. DOI: 10.1038/s41467-020-18520-7